

# IN-FLIGHT CHARACTERISATION OF CRYOSAT-2 REACTION CONTROL SYSTEM

**Stefano Pessina (1), Susanne Kasten-Coors (2)**

(1) Terma GmbH and VCS AG at ESA/ESOC, OPS-GFF

Robert-Bosch-Str.5, 64293 Darmstadt, Germany;

E-mail: Stefano.Pessina at esa.int ; Phone: +49-6151-90-3183

(2) ESA/ESOC, OPS-GFF, address as above

E-mail: Susanne.Kasten-Coors at esa.int ; Phone: +49-6151-90-3914,

**Abstract:** ESA's Earth Explorer CryoSat, launched on the 8<sup>th</sup> of April 2010, is dedicated to precise monitoring of the changes in the thickness of marine ice floating in the polar oceans and variations in the thickness of vast ice sheets.

The Reaction Control System (RCS) of CryoSat-2 is based on cold-gaseous Nitrogen propulsion, using a High-Pressure storage tank, mechanical pressure regulators and Low-Pressure thrusters. The purpose of the RCS is to perform attitude control (generating all the reaction moments in excess of the magnetorquers' capability), attitude manoeuvres and orbit transfer or maintenance.

During CryoSat-2 LEOP, Commissioning and Routine operations phases, different activities were performed by the Flight Dynamics team of the European Space Operations Centre (ESOC), for in-flight characterisation of the RCS: in-flight cold-gas consumption, monitored by two different methods (PVT and Thrusters-activity), mass-flow calibration of the thrusters, force calibration of the orbit-control and attitude-control thrusters.

This paper will focus on these activities, reporting on adopted methods, operational concepts and results, from direct monitoring and analysis of the actual CryoSat-2 spacecraft performances.

**Keywords:** RCS, Gauging, Thrusters, In-flight calibration.

## 1. Introduction

The CryoSat-2 satellite replaces CryoSat, lost during a launch failure in 2005. CryoSat-2 was launched by a Dnepr vehicle from the Baikonur Cosmodrome on the 8<sup>th</sup> of April 2010.

Primary goals of CryoSat are to provide observations for determining the regional and basin-scale trends in perennial Arctic sea ice thickness and mass, and for determining the regional and total contributions to global sea level of the Antarctic and Greenland Ice Sheets. Secondary mission goals of CryoSat are to make observations of the seasonal cycle and inter-annual variability of Arctic and Antarctic and of the variation in thickness of the world's ice caps and glaciers.

The nominal mission duration is 3 years, in a polar low-Earth, non-Sun-synchronous orbit. Due to this, the orbital plane rotates with respect to the sun direction: the nodal plane regresses at a rate of about 0.25° per day, making half a revolution and sampling all local solar times in just over 8 months; therefore the satellite faces great variations in solar illumination.

The spacecraft design is based on a rigid structure without moving parts. The Attitude and Orbit Control System (AOCS) and the Reaction Control System (RCS) provides all functions needed for adequate knowledge of spacecraft attitude during all operational phases of the mission, to accurately maintain and control the spacecraft attitude and its orbit. The attitude is controlled for 3-axis stabilisation; the control reference frame has a "nose-down" configuration with respect to the spacecraft geometric frame, corresponding to 6° rotation around the pitch Y-axis (see Figure 1, where CTRL indicates the control frame).

During orbit-control and coarse-pointing phases, the target attitude is based on the Earth-centric position and the normal to the orbital-plane (respectively Z and Y axis target directions).

During science phases, the Z-axis target attitude is corrected for local-normal pointing with respect to reference Earth ellipsoid; Yaw-steering is used to cope with Earth rotation and ground track direction in Earth-fixed frame (X-axis target direction), resulting in Yaw guidance angle oscillating with respect to the flight direction, from ~0° while over-flying the Earth poles to ~4° at the equator.

The AOCS architecture consists of the following numbers of sensors and actuators:

- 3 Star-Trackers providing high accuracy autonomous inertial attitude determination.
- 2 cold redundant “Doppler Orbit and Radio-Positioning Integration by Satellite” (DORIS) instruments providing near-real-time navigation.
- 1 Coarse Earth-Sun Sensor (CESS) to provide reliable and robust attitude measurements with respect to the sun and earth, for initial acquisition and coarse pointing mode.
- 3 hot redundant fluxgate magnetometers, used for magnetic torquer control and as rate sensor.
- 3 internally redundant magnetic torquers, for compensation of environmental disturbance torques in support of the cold-gas propulsion system.
- a cold redundant propulsion system for attitude control and orbit transfer and maintenance.

The main payload is the SAR Interferometric Radar Altimeter (SIRAL), supported by DORIS and a Laser Retro-Reflector.

## 2. CryoSat-2 Reaction Control System

The Reaction Control System (RCS) of CryoSat-2 is based on cold-gaseous Nitrogen ( $N_2$ ) propulsion, using a High-Pressure storage tank, mechanical pressure regulators and Low-Pressure thrusters. The purpose of the RCS is to perform attitude control (generating all the reaction moments in excess of the magnetorquers’ capability), attitude manoeuvres and orbit transfer or maintenance (see [1]). As from AOCS preliminary dynamics analysis and design (see [2]), the magnitude of air-drag and solar radiation pressure torque is about one order of magnitude lower than the magnetic disturbance torques. Therefore, these torques were no driver for the AOCS control design. However, since they have no correlation with the magnetic field, they cannot be compensated by magnetorquers throughout the orbit; it is therefore necessary to use the thrusters in support of the magnetic torquers, to keep the attitude within the required pointing accuracy.

The cold-gas is stored in a single spherical tank as a high pressure gas (~270 bars at beginning of life) and it flows into a single-stage Pressure Regulator (PR), where this upstream pressure is reduced to a constant (thruster working) low pressure of about 1.3 bar. The regulator remains in lock-up position until a flow demand is initiated by the system (by means of a commanded opening of the thrusters). When a flow demand from the downstream system occurs, the outlet pressure decreases accordingly, depending on the number and kind of actuated thrusters.

The spacecraft is equipped with 4 Orbit Control Thrusters (OCTs, with a thrust level of ~40mN each) and 16 Attitude Control Thrusters (ACTs, providing ~10mN thrust each), arranged in two redundant branches of 2 OCTs and 8 ACTs (see Figure 1, showing the gas exhaust direction for all the thrusters of Branch-A). The two thruster types are mainly identical, with the only difference being the throat diameter, and hence the thrust produced and the mass-flow demand.

Due to precise orbit determination requirements, the attitude-control thrusters’ configuration foresees no ACT thrusters aligned in along-track direction, i.e. along the spacecraft Roll axis. The amount of thruster actuations throughout an orbit is designed to be limited below 10 sec/orbit of accumulated thruster-pair on-time, to keep the orbit disturbances generated by thruster pair imbalances within acceptable limits. The ACTs can be operated in single pulses of 50 milliseconds to 10 seconds duration per activation, they are commanded in closed-loop by the Attitude and Orbit Control System (AOCS), according to measured depointing from the target attitude: 4 thrusters are used for Yaw control, 4 for combined Roll-Pitch control, with control action in Roll and Pitch only commanded exclusively. The Yaw-control thrusters have a thrust direction parallel the Y-axis of the control reference frame, with for the Roll/Pitch control this is parallel to Z-axis. Additionally, an attitude bias can be commanded from ground, so that the ACTs are used both for small and big attitude manoeuvres: the first to eventually correct for OCTs misalignments (during orbit control

operations), for selecting slew direction and for payload calibration, while the second is used for actual execution of Yaw-turn manoeuvres (see [3]).

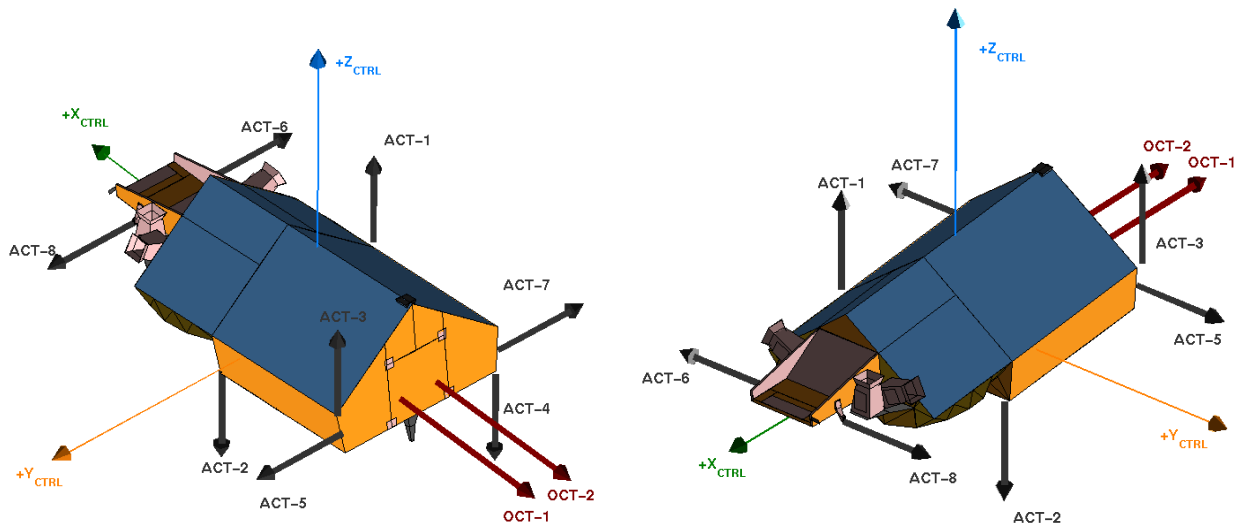


**Figure 1. CryoSat-2 RCS Branch-A: accommodation of the attitude / orbit control thrusters (ACT / OCT). For thrusters, the arrows indicate the gas exhaust direction.**

The OCTs are nominally operated in continuous mode, in open-loop: the timing and duration of actuations is computed on ground, according to  $\Delta V$  needs for orbit acquisition/maintenance. The operational concept for orbit maintenance is based on ground-track control, according to a reference orbit; this is maintained with along-track manoeuvres only (no inclination control). All the OCTs are mounted on the same spacecraft side, with the same thrust direction in body axes, parallel to the positive X-axis of the control reference frame; therefore, the in-flight manoeuvres are executed in forward or backwards flight configuration, in the second case including  $180^\circ$  yaw rotations.

### 3. Flight Dynamics operations at ESOC

At the European Space Operations Centre (ESOC), the Flight Dynamics (FD) Test & Validation (T&V) group is in charge of the FD system check-out during launch preparation activities, from individual software components to system level implementation and team training (see [4]).

In parallel, on-line cross-verification of FD products is provided during LEOP, commissioning and routine operations, together with support for spacecraft in-flight performance monitoring and analysis. To validate the CryoSat-2 FD implementation, T&V has developed dedicated test-tools along with a Flight-Dynamics emulator, based on a high-fidelity modelling of sensors/actuators, spacecraft dynamics and perturbations (see [5], [6]). During CryoSat-2 LEOP, Commissioning and Routine phases, the following activities have been performed by the T&V team to assist Flight Dynamics operations, for in-flight characterisation of the Reaction Control System: in-flight cold-gas consumption, mass-flow calibration of the thrusters, force calibration of the orbit-control thrusters, force calibration of the attitude-control thrusters

### 4. In-flight cold-gas consumption monitoring

The consumption of cold-gas due to autonomous closed-loop attitude control and ground-based open-loop orbit control is monitored by FD team with two different methods:

- PVT method, computing the remaining cold-gas mass from tank pressure/temperature telemetry;
- Thruster-activity method, based on continuous monitoring of commanded thrusters actuation and inlet pressure/temperature state;

During Flight Dynamics system preparation before launch, both methods have been integrated following implementation plans and technical documentation from spacecraft manufactures, and used as is for LEOP operations.

During spacecraft commissioning and routine-phase, the methods have been enhanced by the T&V group, to provide higher accuracy in monitoring capabilities. The progressive refinements with respect to the original implementations are described hereafter.

#### **4.1 Gauging analysis with PVT method (PVT 1)**

The simplest and most applied technique to determine the actual propellant mass is the PVT (Pressure-Volume-Temperature) method. It makes use of existing RCS hardware, by deducing the remaining propellant in the pressure vessel during the mission from housekeeping telemetry.

The physical state of the gas in the tank is obtained from thermistors mounted on the tank structure, together with pressure transducer readings. The tank volume is modelled with linear dependency of the tank pressure.

In order to take into account compressibility effects at high pressure (being the maximum operating pressure of  $\sim 280$  bars), the gas behaviour in the high pressure part has been initially modelled according to real gas equation of state. This was based on a compressibility factor, to be determined according to Benedict-Webb-Rubin equation of state, modified by Lee-Kesler (BWR-LK, see [7]), following the recommended modelling assumptions from the spacecraft manufacturer.

Additionally, the residual Helium (He) in the system is also considered and assumed invariant during mission lifetime: this was estimated during the initial tank loading procedure at launch site (see [11]), using equivalent gas equation of state; the final gas mixture ratio consists of 99,685 %  $N_2$  and 0,315 % He. The total mass of this mixture is calculated to be 36,710 kg (with 36,689 kg of  $N_2$  and 0,021 kg of He). After cross-validation of the final state only, these values have been implemented in FD database for LEOP operations. The properties of the gas mixture are computed on the basis of the pressure/temperature state of the mixture (as from pressure transducer and thermistors reading from telemetry) and the mixture ratio itself, using partial-pressures model (Dalton law), which assumes the gasses to interact in the mixture as ideal gasses.

At beginning of life (BOL), for a pressure of 278.6 bar and a temperature of 15 °C, the worst case error in cold-gas mass estimation can be quantified as follows (see [8]):

- The High-Pressure transducer has an accuracy of 0.11% of the full-scale value (350 bar), considering the acquisition chain and RMS errors, the pressure maximum error is 0.68 bar, corresponding to 0.097 kg error in mass estimation.
- The tank thermistors have an accuracy of 0.25 °C, while the accuracy of the internal gas temperature (with respect to tank mounted thermistors) is 3 °C; considering acquisition and RMS errors, this gives 3.286 °C absolute error, corresponding to 0.46 kg in mass
- The tank volume estimation has an accuracy of 0.1% (i.e. 0.136 litres, 0.04 kg in mass)
- The compressibility factor modelling using BWR-LK equation of state is 0.3%, resulting in 0.124 kg cold-gas mass
- The mixture ratio estimation has an accuracy of 0.22%, giving a mass error of 0.09 kg

The total is  $\sim 0.8$  kg, with almost half of this due to thermal transient and inconsistencies between tank and actual gas temperature.

#### **4.2 Enhanced PVT method (PVT 2)**

In order to improve the overall PVT accuracy, the BWR-LK model has been successively replaced by bi-cubic interpolation of NIST real gas database tables (see [9]). With these tables, the uncertainty in density of the Nitrogen equation of state is 0.02% from temperatures of 240 to 523 K

at pressures less than 300 bar. (see [10]). Helium is modelled as well with the correspondent NIST based look-up tables: the uncertainty of the equation of state is 0.1% between 200 and 400 K.

The N<sub>2</sub>/He mixture ratio was re-computed, analysing all the intermediate steps of the initial tank loading procedure, to provide a new estimation based on the updated real-gas model.

The procedure foresaw an initial condition of the RCS Tank prior Final Tank Loading with gas mixture ratio of 90 % N<sub>2</sub> and 10 % He, as shipped to the launch site. Here, in order to reduce the He part in the final gas mixture the tank has been depressurised to 8.9 bars. The tank has then been filled with gaseous Nitrogen to about 272 bars at 22°C. Considering thermistors and high-pressure transducer reading during this procedure, the initial/intermediate/final states have been re-evaluated using NIST gas model: these gives a mixture ratio of 99.635% N<sub>2</sub> and 0.365% He.

To have a better representation of the physical state of the gas, in particular of its temperature, the analysis of telemetry samples was expanded to all the telemetry available every 24 hours, with sensor data filtering (zero-phase forward and reverse filtering) and statistical mean computation

### 4.3 Cold-gas thruster theoretical model

To reconstitute the mass-flow of the thruster, a theoretical model was used (see [12]), based on these preliminary assumptions:

- cold-gas assumed to be ideal Nitrogen, with constant specific heats
- gas flow is isentropic (i.e. no friction, no heat transfer)
- constant thermodynamics properties on surfaces normal to streamlines
- in the volume comprised between the Pressure-Regulator and thruster inlet: uniform thermodynamics properties, gas velocity (and linear momentum) assumed to be zero
- no boundary layers and transient are considered

With use of conservation laws for mass, linear momentum and energy and the Reynolds' transport theorem, the De Saint Venant's equation can be obtained. This gives the ratio between mass-flow and local section of the nozzle, as function of the local pressure ratio (between inlet and local pressure). The ratio decreases from 1 (at the nozzle inlet) to near zero (nozzle exit surface) and it reaches its maximum in the nozzle throat, where the equation can be written as:

$$\frac{\dot{m}}{A_t} = \left(\frac{1+\gamma}{2}\right)^{(1+\gamma)/(2 \cdot (1-\gamma))} \cdot \sqrt{\gamma} \cdot \frac{P_c}{\sqrt{RT_c}} \quad (1)$$

In this formula,  $\gamma$  is the ratio of specific heats at constant pressure and volume ( $\gamma = C_p/C_v$ ),  $P_c$  and  $T_c$  are the gas pressure and temperature at thruster inlet, while  $A_t$  is the local section area in the nozzle throat. The local expansion ratio gets related to the local pressure ratio, as follows:

$$\frac{A}{A_t} = \frac{\left(\frac{\gamma+1}{2}\right)^{(1+\gamma)/(2(1-\gamma))}}{\sqrt{\frac{2}{\gamma-1} \cdot \left(\frac{p}{p_c}\right)^{2/\gamma} \cdot \left[1 - \left(\frac{p}{p_c}\right)^{(\gamma-1)/\gamma}\right]}} \quad (2)$$

A cold-gas thruster delivers thrust through the expansion of gas through a nozzle. The thrust is created by exchange of linear momentum between the accelerated gas flowing through the nozzle and the pressure difference between both sides of the nozzle exit surface.

Knowing the nozzle geometry (entry, throat and exit areas) and the inlet pressure, one can then solve (2) in an iterative process, to obtain the gas pressure at nozzle exit section,  $P_e$ .

The gas exhaust velocity and the thrust level can be expressed as:

$$V_e = \sqrt{\frac{2\gamma}{\gamma-1} \cdot RT_c \left(1 - \left(\frac{p_e}{p_c}\right)^{(\gamma-1)/\gamma}\right)} \quad (3)$$

Solving the nozzle-exit surface integrals (considered to be part of a sphere of radius  $r$ , delimited by a cone whose apex is at the centre of the sphere and whose half aperture angle is  $\alpha$ ), the thrust expression can be obtained (along the nozzle longitudinal axis  $z$ , considering as well the atmospheric ambient pressure  $P_a$ ):

$$\vec{T} = -\left[\dot{m}V_e \cdot \frac{1 + \cos\alpha}{2} + (p_e - p_a)\pi r^2 \sin^2\alpha\right] \cdot \vec{z} \quad (4)$$

From the Eq. (4), the temperature terms cancel, leaving the thrust independent of temperature, according to the modelling assumptions.

#### 4.4 Cold-gas bookkeeping based on thrusters' activity (method THR Act.1)

This method requires careful observation and logging of all the spacecraft operations during each of ACT activations and OCT manoeuvres which deplete cold-gas. With the duration of the thruster operation and the mass-flow known or estimated, the quantity of propellant used for each thruster can be calculated.

The thruster model of the previous section was used for this method, together with the data about the nozzle geometry; the nozzle throat diameter is different for ACT and OCT (respectively 0.22 and 0.43 mm, to deliver different thrust level), the other geometry parameters are the same: nozzle exit diameter 4.6 mm, nozzle length 8.6 mm (diverging part only), nozzle cone half angle  $15^\circ$ .

Considering the active branch of the RCS, the house keeping telemetry for gas pressure in low-pressure part (thruster inlet), the individual temperatures and the commanded pulses of each thruster are collected analysing continuous data from mass-memory dumps. The data then need to be synchronised due to difference data-pool acquisition and frequency of received telemetry.

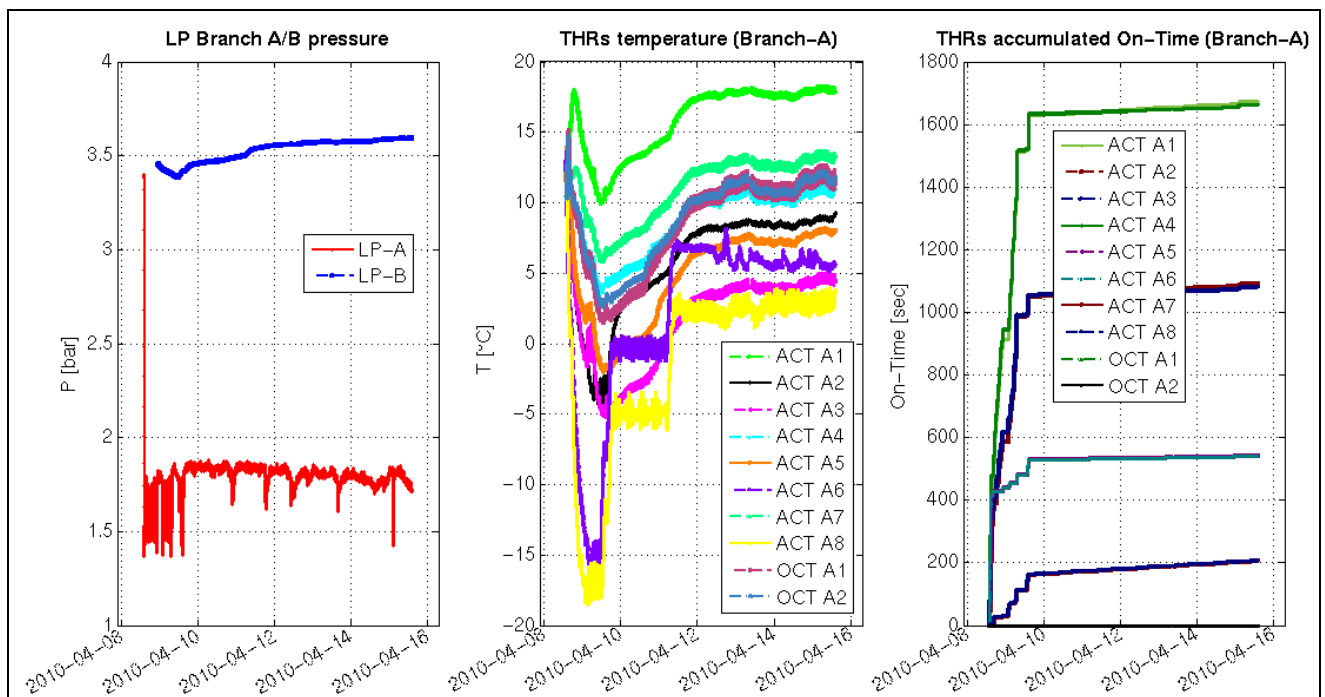


Figure 2. LP Pressure, Temperature, thrusters' accumulated On-Time; 1<sup>st</sup> week of operations

Figure 2 shows the data collected over the first week of in-flight operations from launch, for the individual thrusters' pressure, temperatures and commanded on-time of the active RCS branch (together with LP pressure of B branch): in the central plot the initial cooling after separation and the successive activation of thermal controls is evident; in the side plots, it is possible to note the intense thrusters activity during LEOP, due to initial rates damping after separation from the launcher upper-stage and the AOCS mode changes, prior to reaching the science mode.

The method is affected by the accuracy of the mass-flow estimation, of the low-pressure transducer and thermistors readings, while the errors in On-time reporting are negligible.

Additionally, the monitoring needs to run continuously and eventual telemetry gaps can affect the final state estimation. Since this bookkeeping method uses an integration of predicted propellant flow rates, the errors related to the calculation of remaining propellant accumulate over mission life.

#### **4.5 Enhanced cold-gas bookkeeping based on thrusters activity (method THR Act.2)**

The following enhancements were considered to improve the accuracy of the originally implemented bookkeeping method.

For a better estimation of the pressure transients during thrusters' actuation (when the regulator is at soft lock-up pressure because of prolonged closure of the thrusters), the low-pressure telemetry readings were changed from hardware based telemetry (0.25 Hz frequency) to AOCS monitoring telemetry (1 Hz frequency), considering also more accurate calibration curves, from raw to engineering units. Moreover, accurate data interpolation was considered when synchronising the telemetry parameters coming from different packets and having diverse sampling frequencies.

Then, the acceptance test results of the thrusters (see [13]) were considered: a test campaign has been run prior to launch for each of the thrusters, characterising thrust level and mass-flow at a reference pressure of 1.45 bars for all the units installed on the spacecraft. For one ACT and one OCT, the dependency to various inlet pressure levels was also analysed (range from 1.3 to 2.5 bars). Combining this information and assuming the pressure dependency to be applicable for all units, it was possible to compute correction coefficients for both thrust and mass-flow, using the test conditions, to be applied to the thruster analytical model.

#### **4.6 Summary of cold-gas consumption and mass-flow calibration**

Figure 3 shows in the left plot the results of the various methods used for cold-gas consumption, based on weekly data analysis of the telemetry available from launch until 2011/01/24.

The big jumps are due to the execution of orbit control manoeuvres; this is evident in the period between May and July 2010, when the manoeuvre sequence for acquisition of the reference orbit was executed (see Table 1 in Section 6).

As it can be seen, the enhancements introduced both for the PVT and THR-activity methods have reduced the relative drift between them (see right plot of Figure 3): indicating with  $\Delta_1$  and  $\Delta_2$  the difference in estimated cold-gas consumption between PVT and THR-activity, respectively before and after introducing modelling improvements, these maximum differences have been reduced from 180 grams to less than 25 grams for each of the weekly estimations, while the mean difference reduces from 121.3 grams to 16.8 grams.

### **5 Thrusters mass-flow calibration**

Given the results from the steps above and to further eliminate the accumulated errors in the mass-flow modelling for the thruster activity bookkeeping ("THR Act.2"), an individual thrusters' mass-

flow calibration cross-calibration was performed, with a constrained linear least-squares solver, using the reconstituted N<sub>2</sub> mass from the “PVT 2” method as reference.

The algorithm is based on computation of accumulated mass consumption for each day of the mission to compute final fitted calibration coefficients for each of the thrusters.

We call “x” the vector containing the mass-flow calibration for each thruster of the active RCS branch, of dimension [10x1], with initial guess corresponding to 1 in each element. Then, the algorithm solves the linear system  $C \cdot x = d$  in the least-squares sense, without additional linear constraint (of the kind  $A \cdot x \leq b$  or  $A \cdot x = b$ ), but setting upper and lower boundaries to the solution.

The boundaries has been set to 5% correction factor (e.g.  $0.95 < x < 1.05$ ).

The matrix “C” contains the mass-consumption from THR-activity for each thruster accumulated in each of the N analysed days (dimension [Nx10]), either because of attitude control, slew manoeuvres (ACTs only) or orbit manoeuvres (using OCTs). The vector “d” contains the daily accumulated mass consumption (dimensions [Nx1]) according to PVT method, given by the difference of the initial tank filling condition with daily estimated mass.

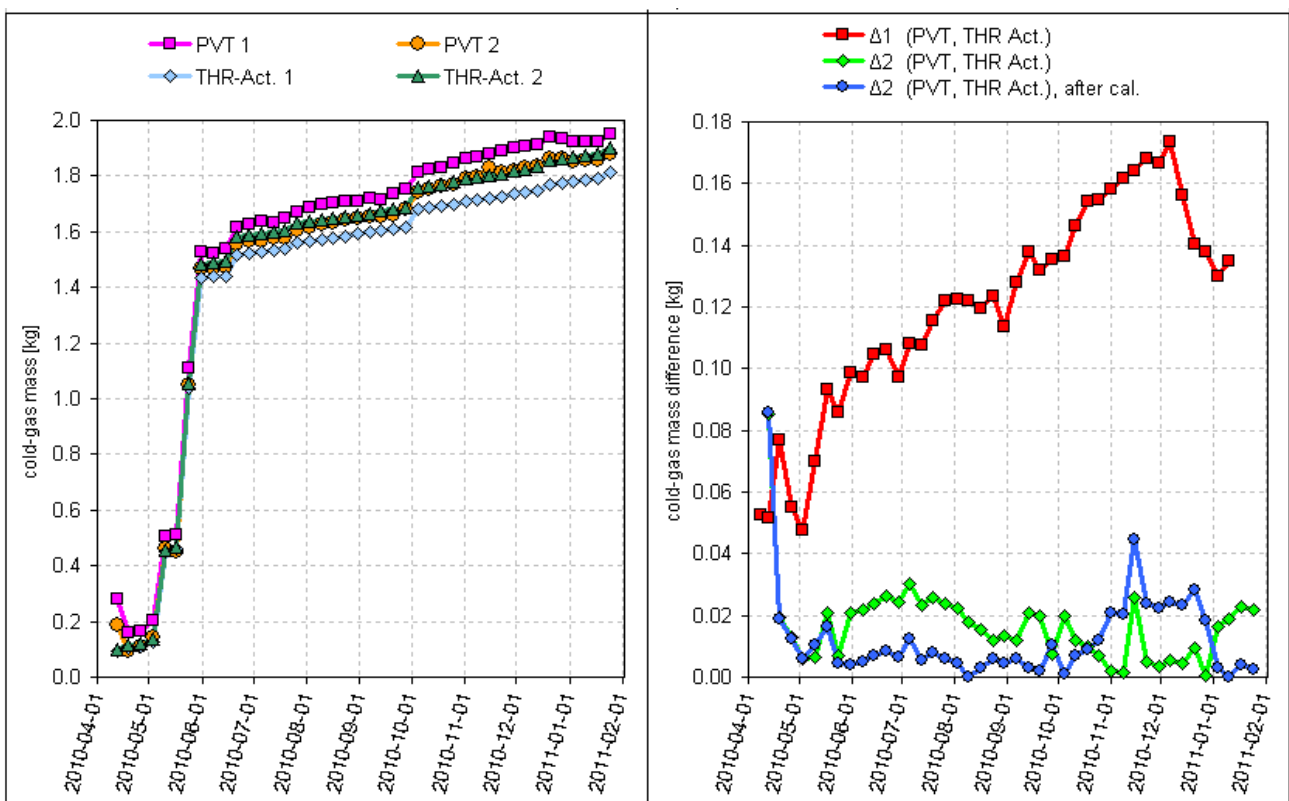


**Figure 3. Cold-gas mass consumption (weekly) with PVT and thruster activity methods**

The results of the mass-flow calibration are all below 1% with exception of OCT-1 thruster:

ACT-1	ACT-2	ACT-3	ACT-4	ACT-5	ACT-6	ACT-7	ACT-8	OCT-1	OCT-2
0.9993	0.9994	0.9985	0.9976	0.9950	0.9955	0.9996	0.9996	0.9778	0.9965

This is due to the fact that the optimisation has been performed without any equality constraints, thus the effect of the calibration is to level-out the un-balance between thrusters actuated together, as determined with on-ground unit testing. To take this into account, a new optimisation is performed, forcing equality constraints for the positive/negative Yaw control thrusters (meaning imposing the mass-flow of ACT-5&6 equal to each other; same for ACT-7&8) as well as for the orbit control thrusters (OCT-1&2).

The final calibration factors obtained are hereafter reported, as it could be expected, the calibrated mass-consumption doesn't differ from the previous run:

<b>ACT-1</b>	<b>ACT-2</b>	<b>ACT-3</b>	<b>ACT-4</b>	<b>ACT-5</b>	<b>ACT-6</b>	<b>ACT-7</b>	<b>ACT-8</b>	<b>OCT-1</b>	<b>OCT-2</b>
0.9993	0.9994	0.9985	0.9976	0.9953	0.9953	0.9996	0.9996	0.9871	0.9871

In the right plot of Figure 3, the difference between “PVT-2” and “THR Act.2” after use of the computed mass-flow calibration factors is shown: it can be seen that there is an overall improvement, with the mean difference reducing from 16.8 grams to 12.4 grams. The residual discrepancies between the methods can be now well correlated to the thermal transient experienced by the spacecraft (due to difference in mean Sun illumination, originating spacecraft-wise thermal transient at the beginning of the mission and from October-2010 to January 2011), when the PVT method has reduced accuracy.

## 6. Force calibration of the Orbit-Control Thrusters

The force calibration of the OCT is necessary to evaluate the executed orbit-control manoeuvres and to improve the accuracy in planning the successive ones, thus in computing on-ground the duration of the thrusters’ opening time, in order to achieve the target  $\Delta V$ . At the time of writing, 25 manoeuvres have been executed to cope with different mission needs.

**Table 1. Orbit control manoeuvres overview**

ID	Purpose	Start Time [UTC]	Duration [sec]	Target $\Delta V$ [m/sec]	ORB.DET. Perf. factor
1	RCS commissioning	2010-04-15T17:46:30Z	60	0.006578	0.8398
2	Acquisition of ref.orbit	2010-05-03T17:54:31Z	120	-0.01145	0.9924
3	Acquisition of ref.orbit	2010-05-04T00:29:43Z	300	-0.02864	0.9821
4	Acquisition of ref.orbit	2010-05-04T18:37:59Z	600	-0.05681	0.9919
5	Acquisition of ref.orbit	2010-05-05T17:43:41Z	900	-0.08592	0.9814
6	Acquisition of ref.orbit	2010-05-06T18:26:05Z	1500	-0.1428	0.9818
7	Acquisition of ref.orbit	2010-05-18T00:42:22Z	899	0.084	0.9972
8	Acquisition of ref.orbit	2010-05-18T04:00:41Z	898	0.084	0.9912
9	Acquisition of ref.orbit	2010-05-18T23:50:36Z	898	0.084	0.9861
10	Acquisition of ref.orbit	2010-05-19T03:08:55Z	898	0.084	0.9804
11	Acquisition of ref.orbit	2010-05-20T00:38:04Z	898	0.084	0.9765
12	Acquisition of ref.orbit	2010-05-20T03:56:23Z	898	0.084	0.9717
13	Acquisition of ref.orbit	2010-05-20T23:46:19Z	913	0.084	0.9837
14	Acquisition of ref.orbit	2010-05-27T00:27:11Z	932	-0.084	1.01
15	Acquisition of ref.orbit	2010-05-27T03:45:24Z	932	-0.084	0.9934
16	Acquisition of ref.orbit	2010-05-28T01:14:23Z	939	-0.084	1.00
17	Acquisition of ref.orbit	2010-05-28T04:27:45Z	1397	-0.125	0.9978
18	Acquisition of ref.orbit	2010-06-15T03:01:57Z	762	0.068	1.003
19	Acquisition of ref.orbit	2010-06-18T01:14:01Z	39	0.0035	0.9546
20	Venting of B-branch	2010-07-20T12:36:59Z	1	-0.0004	0.5204
21	Collision Avoidance	2010-10-02T03:00:42Z	224	-0.02	0.9892
22	Collision Avoidance	2010-10-02T07:27:07Z	254	0.0226	0.985
23	Routine Orbit Trim	2010-10-28T06:32:39Z	34	0.003	1.012
24	Routine Orbit Trim	2010-12-16T03:06:45Z	155	0.014	0.9731
25	Routine Orbit Trim	2011-01-21T10:04:40Z	153	0.0135	1.008

After separation from the launcher’s upper-stage and conduction of LEOP and initial commissioning operations (involving also a test manoeuvre for RCS commissioning), CryoSat-2 acquired its reference orbit for science phase, implementing a series of orbit control manoeuvres (see [15]).

During routine-operations, the orbit control strategy is based on a reference orbit with an equidistant node crossings distribution, with a repeat cycle of 369 nodal days. The distance of the operational orbit with respect to the reference orbit is measured as perpendicular distance in ground-track at the Equator crossings. Each control cycle is based on specific assumption of the satellite drag coefficient, with crossing time controlled against a dead-band of +/- 1km.

Additionally, the proximity with other satellites and space debris is monitored continuously; such that in case a proximity warning is issued, a collision avoidance strategy is executed (composed of 2 manoeuvre of similar magnitude in opposite directions).

Venting manoeuvres are necessary to prevent an excessive increase of pressure in the inactive RCS branch (as an example, see LP build-up in Branch-B, in the leftmost plot of Figure 2).

Table 1 gives an overview of all the 25 orbit manoeuvres implemented so far, distinguishing the different purpose of manoeuvring explained above. The table indicates also the execution time, the commanded on time for each of the OCTs, the target  $\Delta V$  (negative indicates anti-flight manoeuvre) and the performance factor estimated after the manoeuvre by orbit-determination activities.

When a specific orbit transfer is required or when a constraints' violation is foreseen, the FD orbit subsystem optimises a target  $\Delta V$  for orbit correction together with the execution time (defined as angular separation from a specific ascending node crossing); this is to be executed as an actuation of the 2 OCTs of the RCS branch in use.

Due to the lack of inclination control, the planned  $\Delta V$  is either towards in-flight direction (default nominal pointing) or anti-flight, thus requiring a  $180^\circ$  yaw-turn before and after the execution of the manoeuvre. The execution of manoeuvres anti-flight requires a proper planning for direction and timing of the slew manoeuvre, in order to avoid multiple blinding of the Star-Trackers (from the Sun and the Moon): the selection of the sensors priority sequence I commanded from ground, to instruct the AOCS about which Star-Trackers should be used in case multiple attitude sets are available, according to blinding opportunities.

The orbit-control manoeuvre is then implemented as follows: based on the monitoring of the latest available telemetry from the RCS, the temperature and pressure of both the high-pressure and low-pressure part of the system are logged and used to predict the condition for the manoeuvre execution. Specifically, it is necessary to model the regulated low-pressure during the manoeuvre (inlet condition of the thrusters) to predict the thrust level, being this in a first approximation not dependant on the temperature conditions of the gas, as from Eq. (4). It is then possible to compute the On-Time to be commanded on-board using the rocket equation (the dependency on mass-flow is here negligible, due to the specific impulse magnitude of  $70\pm 5$  seconds in the thrusters' operative range).

During commissioning and routine phases, different models for the regulated-pressure were analysed, progressively refining them according to observations: for the very first manoeuvre, the LP-pressure was taken from manufacturer documentation, as expected constant value; successively, its value was retained from the previous manoeuvres, as future prediction; then, a correlation between regulated pressure and High-Pressure tank value was supposed (from Manoeuvre 14).

The currently assumed model (introduced in the last manoeuvre) foresees the prediction of the regulated pressure based on the cold-gas density in the High-Pressure part: the LP pressure value is monitored thanks to housekeeping telemetry in the interval around the manoeuvre. With parallel analysis of the on-board commanded On-Time for the OCT, it is possible to identify and isolate the LP pressure transducer readings and to compute their mean value during the OCT opening time (using trapezoid numerical integration).

Figure 4 (left plot) shows the correlation between the gas density in the tank and the reconstituted mean-regulated pressure during OCT operations: the plot indicates as well the progressive number of each of the executed manoeuvres, together with a linear fit of the data. Manoeuvres number 3 and 20 have been excluded from this analysis, respectively because a telemetry gap occurred (therefore the system state during the manoeuvre cannot be assessed) and because of extremely short duration (1 sec, executed only for B-branch venting), in the latter making potentially very inaccurate the system characterisation, due to transients.

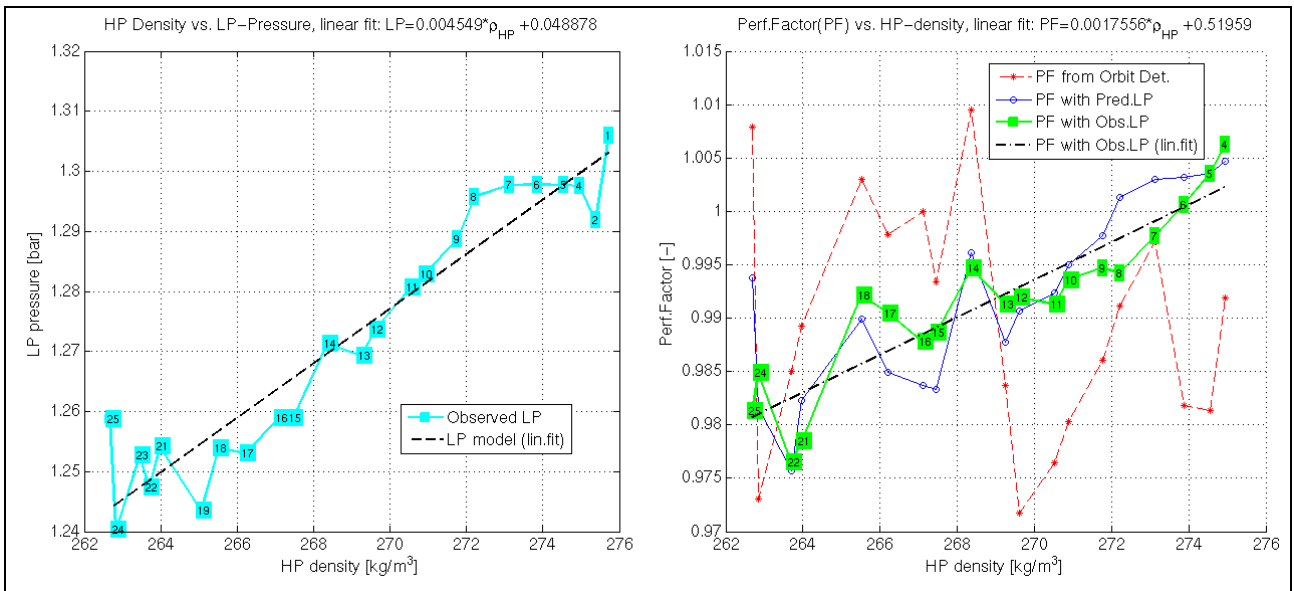


**Figure 4. Low-Pressure, Performance-Factor as function of gas density (tank), in OCT ops**

Thanks to the stable AOCS pointing during orbit control manoeuvres and to the continuous operation of OCTs in parallel direction, the thruster calibration is performed in a traditional way: the along-track component of the spacecraft acceleration can be determined from radiometric data, eventually augmented by DORIS navigation packets.

This is compared with the planned acceleration profile, to derive a performance factor (PF) for both thrusters ( $PF_{\text{Orb.Det.}} = \Delta V_{\text{Orb.Det.}} / \Delta V_{\text{Plan}}$ ). In order to evaluate the actual performance of the thrusters, eliminating the error due to the RCS state prediction, the manoeuvre are re-estimated using the commanded On-time, first re-computing the LP prediction based on the actual cold-gas density during the manoeuvre ( $PF_{\text{Pred.LP}} = \Delta V_{\text{Orb.Det.}} / \Delta V_{\text{Pred.LP}}$ ), then using the monitored LP pressure, instead of its predicted value ( $PF_{\text{Obs.LP}} = \Delta V_{\text{Orb.Det.}} / \Delta V_{\text{Obs.LP}}$ ).

Figure 4 (in the right plot) shows a summary of the 3 different performance factors. Here, only the manoeuvres with duration  $> 120$  sec are considered, because they can be estimated with higher accuracy by orbit determination techniques. As it can be seen, the overall accuracy of all these manoeuvres with respect to the original plan has been within  $\pm 2\%$  with respect to a mean under performance value of 0.99. Removing the error in Tank state prediction ( $PF_{\text{Pred.LP}}$ ) and then in regulated pressure modelling (in  $PF_{\text{Obs.LP}}$ ), the OCTs thrust-level performance shows a progressive change (with good linearity) from about 1 at beginning of the mission till 0.98 (meaning 2% underperformance with respect to the FD thrusters' model, for identical inlet conditions).

## 7. Force calibration of the Attitude-Control Thrusters

For CryoSat-2 different attitude manoeuvres were executed during commissioning and routine operations: small Roll/Pitch bias angles were used for instrument calibration (with respectively a maximum magnitude of  $0.4^\circ$  and  $0.25^\circ$ ), while  $180^\circ$  Yaw manoeuvres were used for the execution of anti-flight orbit control manoeuvres (and to return to the nominal pointing).

The AOCS performs attitude manoeuvres by means of an attitude bias with respect to the reference attitude. In case of yaw turns while in orbit-control mode, the attitude manoeuvres are executed with trajectory guidance, computing a feed-forward torque for starting and ending the manoeuvre, while controlling the angular velocity at  $0.1^\circ/\text{sec}$  for the yaw rotation, meaning that a slew of this kind is nominally completed in 30 minutes.

The AOCS selects the yaw slew direction taking the minimum angular distance with respect to the target biased reference, when the attitude bias telecommand is processed on-board. If this is  $180^\circ$ ,

there is uncertainty in the slew direction, which is solved on-board according to pointing performances at slew start time.

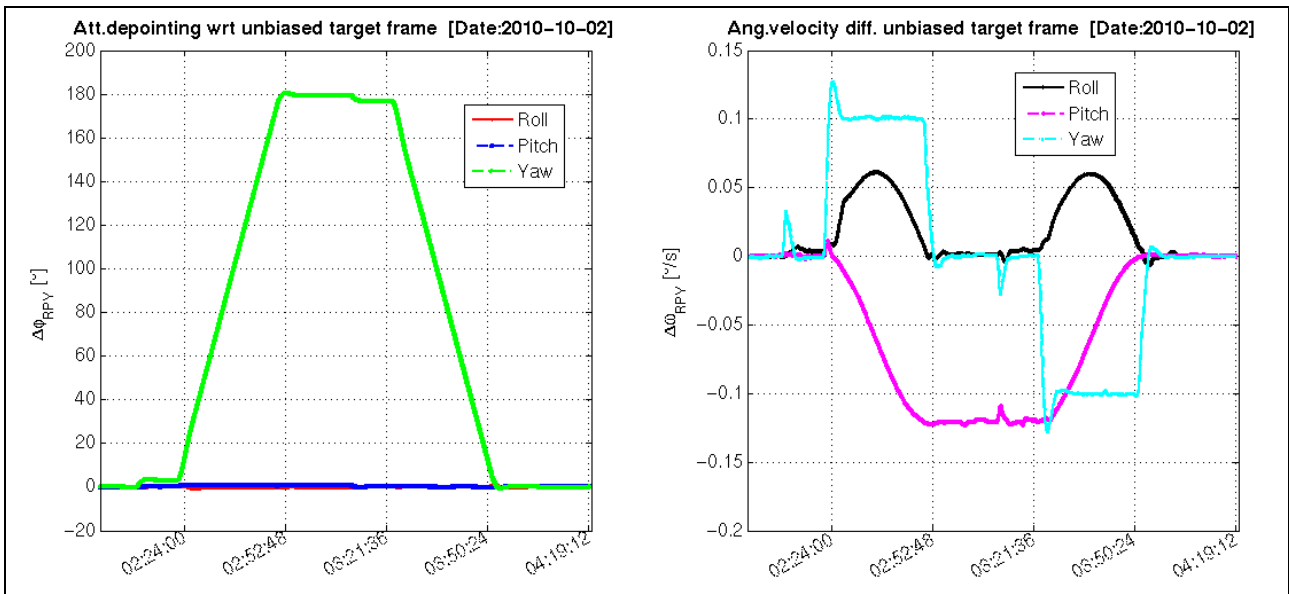


**Figure 5. Attitude dynamics (pointing/rates errors) during the 2 yaw-turns on 2010/10/02**

In order to control on-ground the Yaw-turn direction, the attitude bias is therefore divided in an initial small bias, towards the target direction, and an additional bias, with the remainder of the Yaw turning angle (a split  $3^\circ/177^\circ$  was used so far; this will change to  $0.5^\circ/179.5^\circ$  in future, to reduce the thrusters' activity when acquiring/keeping the intermediate attitude bias).

In order to point the spacecraft for orbit control manoeuvres execution (see Table 1), 6 yaw turns were executed during CryoSat-2 operations at the time of writing (see Table 2).

**Table 2. Yaw-turn manoeuvres overview**

ID	AOCS Mode	Start Time [UTC]	Bias Sequence [deg]	Slew Direction	Final direction of $+X_{CTRL}$
1	Fine-Pointing	2010-04-26T12:44:30Z	180°	N/A	Anti-flight
2	Orbit-Control	2010-05-10T14:00:00Z	+177°, +3°	Positive Yaw	In-Flight
3	Orbit-Control	2010-05-26T13:49:00Z	+3°, +177°	Positive Yaw	Anti-flight
4	Orbit-Control	2010-05-28T13:38:00Z	-177°, -3°	Negative Yaw	In-Flight
5	Orbit-Control	2010-10-02T02:10:22Z	+3°, +177°	Positive Yaw	Anti-flight
6	Orbit-Control	2010-10-02T03:11:36Z	+177°, +3°	Positive Yaw	In-Flight

Figure 5 shows the attitude dynamics evolution (Roll-Pitch-Yaw depointing angles and angular rates errors with respect to local-orbital frame) as observed from telemetry monitoring, during manoeuvres 5 and 6: for executing the 1<sup>st</sup> of the 2 collision-avoidance manoeuvres in October 2010, these involved slewing to  $+180^\circ$  and backwards to 0 yaw bias (both with intermediate bias configuration, according to slew direction planning).

While performing attitude manoeuvres 8 ACTs are actuated in matched pairs, to provide 3-axis torque action with minimum residual force; unbalanced thruster performances can anyway cause a residual  $\Delta V$ . This effect was observed during FD operations, as increased residuals in the orbit determination process around the execution of  $180^\circ$  Yaw manoeuvres (from tens to hundreds of meters RMS). It was therefore decided to characterise the thrust level of the ACTs, combining observations from orbit determination and attitude monitoring functionalities.

Different orbit determinations were run with NAPEOS (Navigation Package for Earth Observation satellites, see [14]), using as observables the S-band radiometric data (antenna angle and Doppler measurement for the Kiruna and Svalbard ground stations), and DORIS data for cross verification of the orbit solution. Given the slew start and end time, the numerical fit is then performed modelling the slew as continuous manoeuvre and assuming as solved-for parameters the Drag-coefficient and the three components of the spacecraft acceleration due to the slew in the “Local-Orbital Frame”. Given the orbital states in Inertial frame (position and velocity in mean equatorial of J2000), the “Local-Orbital Frame” is defined as Radial (parallel to geocentric position), Cross-Track (parallel to the direction normal to the orbital plane, given by the cross product of position and velocity) and Along-Track (to complete a right-handed triad). Knowing the mass of the spacecraft and the assumed duration (30 min), an equivalent  $\Delta V$  can be estimated with NAPEOS in this frame ( $\Delta V_{OD}$ ), to fit the observables of the Orbit-Determination process.

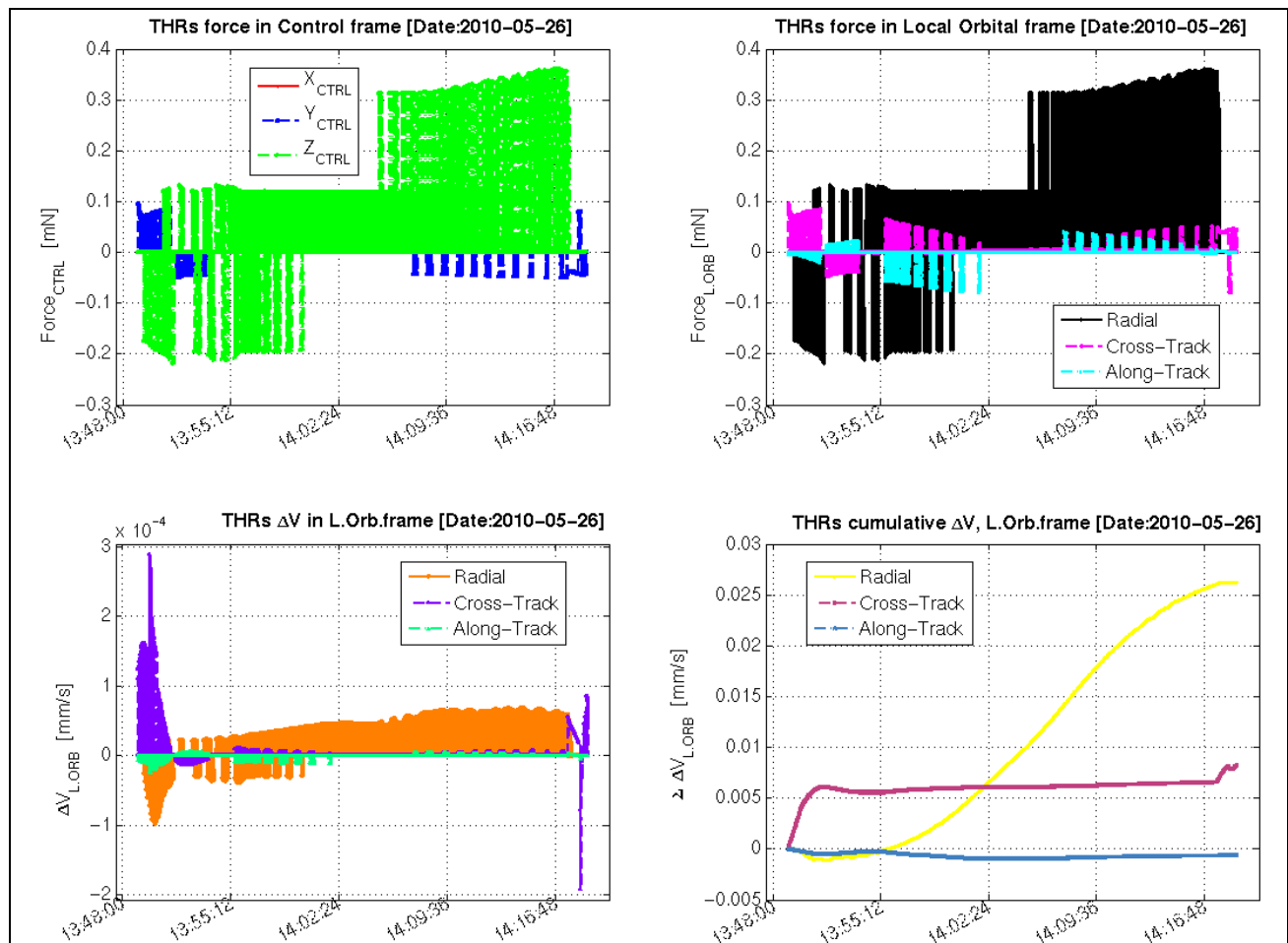


**Figure 6. Progressive steps in the computation of the accumulated  $\Delta V$  due to ACT actuations, during  $180^\circ$  yaw turns (test case, manoeuvre-3 on 2010-05-26)**

On the attitude monitoring side, for each slew, the telemetry is analysed to collect the Low-pressure part physical state (pressure/temperature) and ACT commanded On-Times, with the same software functionalities used for running the bookkeeping analysis based on thruster activity (see Figure 2).

The procedural steps were the following:

- The thrusters’ model based on the Eq. (4) is assumed, together with the correction from on-ground unit testing (as mentioned in Section 4.5), using LP pressure from telemetry as an input. Knowing the thrusters’ alignments in Control frame (see Figure 1), it is possible to obtain the total force due to attitude control thrusters’ actuation: this is done considering their open/close status from telemetry and the reconstituted force-level, summing the contribution when matched-pairs pulses are executed (see Figure 6, top-left plot).

- During the execution of the slew, the actual pointing performances differ of few degrees with respect to a linear propagation of the commanded bias angles at constant angular velocity (see Figure 5). In order to obtain the spacecraft pointing, the Star-Tracker telemetry is then processed, converting the attitude packets to depointing errors in the Local-Orbital frame. These angles are then interpolated to the instant when each of the thrusters' pulses have been executed, so that it is possible to convert the residual force from spacecraft-fixed control frame (CTRL) to Local-Orbital frame (L.ORB) for each of the actuated pulses (see Figure 6, top-right plot).
- Knowing the mass of the spacecraft and the duration of the force action, reported in telemetry by the commanded pulses, it is possible to convert the force profile to a sequence of  $\Delta V$  in Local-Orbital frame (see Figure 6, bottom-left plot).
- The cumulative sum of all the  $\Delta V$  gives at the very end of the slew ( $\Delta V_{AM}$ ) the reconstituted total effect of the un-balanced thruster levels due to ACT actuation, for the assumed thruster models and monitored attitude (see Figure 6, bottom-left right).
- The final  $\Delta V_{AM}$  coming from attitude monitoring and on-ground thruster models is then compared with the residual from the orbit determination, to derive single thrusters' performance factor. In order to do this, the  $\Delta V_{OD}$  has to be scaled down to  $\Delta V_{OD-eqv}$ , using the ratio between the slew duration assumed for fitting the profile and the actual ACT total On-Time (sum of the On-time of each pair). As the problem is over-determined (eight force calibration factors unknown, three  $\Delta V$  components), it is solved minimising a constrained nonlinear multivariable function: the constraints are imposed to keep (with margin) the calibration factors within the expected thrusters performances ( $\pm 7\%$  with respect to the on-ground measured thrust-).

Among all executed yaw-turns (see Table 2), manoeuvre 5 and 6 were executed too close to an orbit control manoeuvre: this left no dedicated determination arcs for specifically estimating the residual  $\Delta V$  due to ACTs operations only. When optimising the performance-factors to fit each of the manoeuvres 1, 2, 3 and 4, it is possible to obtain very good solutions (reconstituted  $\Delta V_{AM}$  using the determined calibration factors was less than 1% in magnitude and  $0.1^\circ$  depointing with respect to  $\Delta V_{OD-eqv}$ ). Considering that manoeuvre 1 was a test manoeuvre, executed in AOCS mode "Fine-Pointing" (afterwards the "Orbit-Control" mode was assumed as baseline, due to better performances in big-attitude manoeuvre execution), manoeuvres 2 and 3 were selected for ACTs force-level cross-calibration, being representative of both slew to anti-flight configuration, and backwards to in-flight nominal pointing. The following table shows the accumulated thrusters on-time and the above-mentioned  $\Delta V_{OD-eqv}$  for these two slews:

Accumulated Thrusters' On-Time [sec]								Orbit-Det. $\Delta V_{OD-eqv}$ [mm/s]		
ACT-1	ACT-2	ACT-3	ACT-4	ACT-5	ACT-6	ACT-7	ACT-8	Radial	Along-T	Cross-T
124.9	3.8	20.4	141.5	47.1	47.1	70.6	70.6	0.0084	0.0059	-0.0023
10.8	143.2	148.7	16.4	68.2	68.2	49.7	49.7	0.0262	0.0101	0.0002

The procedure described above was run for these 2 manoeuvres (e.g. see Figure 6 for a break-down of the steps for Slew-3), summing the total  $\Delta V$  deviation as the target function to minimise, the following set of ACT force-level calibrations factors can be obtained:

ACT-1	ACT-2	ACT-3	ACT-4	ACT-5	ACT-6	ACT-7	ACT-8
1.0122	0.9954	0.9796	1.0128	0.9961	1.0039	0.9981	1.0019

These calibrations allow reconstituting both target  $\Delta V$  within 3% of its magnitude and  $10^\circ$  of its direction.

## 8. Conclusions

In this paper, different activities have been presented related to the in-flight characterisation of the CryoSat-2 Reaction Control System.

From the cold-gas gauging analysis, the operational results from the PVT and thruster-activity methods have been reported, indicating as well progressive adjustments towards increased accuracy in both methods, including cross-calibration process of the consumed mass, which allowed the characterisation of the mass-flow for attitude and orbit control thrusters.

Analysing the orbit-control manoeuvres, both the behaviour of the mechanical pressure regulator and the OCTs force factor has been determined, as function of the gas density stored in the tank.

Additionally, combining orbit determination and attitude monitoring functionalities, it was possible to characterise the performance factor of the attitude control thrusters, for all considered slews separately, and for two of them as cross-calibration test-case.

All the operational concepts developed within CryoSat-2 initial mission life-time will be further developed as long as new calibration opportunities will arise.

Further works could involve additional improvements in the pressure-regulator performance prediction (for better planning of orbit control manoeuvres) and in the characterisation of orbit disturbances while performing long slew manoeuvres.

Even considering mission specific constraints, most of these concepts could be adopted for in-flight characterisation of the Reaction-Control System of future Earth–Observation satellites that will be operated at ESOC (SWARM, ADM-Aeolus).

## 9. References

- [1] EADS-Astrium tech. report, "CryoSat-2 Users Manual", CS-MA-DOR-SY-0001
- [2] EADS-Astrium tech. report, "CryoSat Satellite Dynamics Analysis", CS-TN-DOR-SY-0014
- [3] EADS-Astrium tech. report, "CryoSat AOCS S/W Requirements", CS-RS-DOR-DC-0003
- [4] Pessina S.M., Tucci L., Flegel M.L., Kasten-Coors S., "ESOC flight dynamics LEOP, commissioning and routine operations preparation for the GOCE mission", 21<sup>st</sup> International Symposium on Space Flight Dynamics (ISSFD2009), Sept.2009, Toulouse, France
- [5] Pessina S.M., Tucci L., Kasten-Coors S., Flegel M.L., "ESOC precise flight dynamics emulation for the GOCE mission", 58<sup>th</sup> International Astronautical Congress, Sept.2007, Hyderabad, India,
- [6] Pessina S.M., Tucci L., Kasten-Coors S., "ESOC Flight Dynamics precise emulators for CryoSat, Herschel, Planck: development and applications", 25<sup>th</sup> International Symposium on Space Technology and Science (ISTS), June 2006, Kanazawa, Japan; ISTS 2006-t-09;
- [7] Lee B.I., Kesler M.G., "A generalized thermodynamic correlation based on three-parameter corresponding states", American Institute of Chemical Engineering Journal, 21, 510-527, 1975.
- [8] EADS-Astrium tech. report, "CryoSat RCS Gauging Analysis", CS-TN-DOR-SY-0059
- [9] NIST Chemistry WebBook, "NIST Standard Reference Database Number 69", "Thermophysical Properties of Fluid Systems", <http://webbook.nist.gov/chemistry/fluid/>
- [10] Span, R.; Lemmon, E.W.; Jacobsen, R.T.; Wagner, W.; Yokozeki, A., "A Reference Equation of State for the Thermodynamic Properties of Nitrogen", J. Phys. Chem. Ref. Data, 2000, 29, 6
- [11] McCarty, R.D.; Arp, V.D., "A New Wide Range Equation of State for Helium", Adv. Cryo. Eng., 1990, 35, 1465-1475
- [12] Marc X., "CryoSat RCS Model", ESOC Flight Dynamics Division, internal Technical-Note
- [13] Marotta UK Ltd, "CryoSat-2 FM Thruster Performance Summary" C2-TN-PAL-RU-6004
- [14] Garcia Matatoros M. A., Kuijper D., Righetti P. L., "NAPEOS: ESOC NAPEOS: ESOC Navigation Package for Earth Observation Satellites" , European Workshop on Space Flight Dynamics Facilities, Sept. 2003, Darmstadt, Germany
- [15] Martin Serrano M.A., Merz K., Ziegler G., "Cryosat-2: from LEOP to acquisition of the reference orbit", ISSFD2011, March 2011, São José dos Campos, Brazil